International Journal of Engineering and Advanced Technology (IJEAT)
ISSN: 2249-8958 (Online), Volume-9 Issue-2, December, 2019

# Design of Multi-loop Current Control Strategies for LCL Filtered Grid-connected PV System

**Pradeep Kumar Sahu, Satyaranjan Jena, Geetanjali Dei**

***Abstract:*** ***This paper presents numerous feedback current controller methods for the grid-connected PV systems incorporating with third order LCL filter. The various potential dual-loop feedback current controller schemes for a grid-tied electrical converter and a comparison among these controllers are made based on their performance. The effectiveness of these current controllers are based on various views like performance under polluted grid condition and also the dynamic performance of two control schemes under different transient conditions. A commonly used PI controller are employed in all cases of multi-loop controllers and also the electrical converter used here is operated in voltage control mode. In this work, a third-order low-pass LCL filter is employed to minimize the high order harmonics which are created due to the switching of the converter. The LCL filter is incorporated among the dc-ac converter and the utility grid. Two current regulation techniques are focused here. The design, analysis and the performance of these controllers are briefly discussed in this paper. By comparing their performance, anyone can suggest their applications in the grid-tied PV systems. All the current control schemes are incorporated with a grid-connected system of 2-KVA voltage source inverter. Simulation results are produced to validate the performances of two current control schemes. The output ohmic resistance of VSI is taken into account here for their performance analysis.***

***Keywords :*** ***Voltage source Inverter (VSI), Low-pass LCL filter, Grid-connected PV system, Dual-loop current control schemes, power quality.***

## I. INTRODUCTION

In present days, renewable energy based distributed generation (DG) systems have been gaining popularity due to environmentally neutral, silently availability, low cost, and and restricted availability of conventional fuels [1]. Solar PV energy sources are the most auspicious renewable energy supply for Indian scenario among the above mentioned energy sources as it is plenty accessible in nature and no adverse effect on the environment. Therefore, Solar PV plants may fulfill the total energy demand of any country in the close to future. A solar PV plants may be functioned in stand-alone mode or grid-tied mode. A grid-tied mode of operation is commonly used in the renewable energy system [1],~[2]. Generally, Voltage source inverter (VSI) plays a crucial role as the power conditioning unit which is required for integrating this renewable source with the grid [3]. All switching harmonics generated by the voltage source inverters can be eliminated by incorporating various low pass filters like *L*, *C*, *LC*, *CL* or *LCL* [4],~[5]. Among all available switching techniques, the sinusoidal pulse width modulation (SPWM) technique is commonly used for voltage source inverter due to its easy real-time implementation and simple structure [4],~[5].

The power conditioning units like step-up dc to dc converter and VSI plays a vital role in the renewable energy systems. These converters are generally used for interfacing among the solar plant and the real grid system. In the current scenario, dual-stage, single-phase, grid-ties solar power generation system architecture is the point of attraction from institution and business sectors because of its simple structure, high power density, more reliability, and plug-and-play features. The first stage is a dc power conditioning step which consists of a dc-dc step up converter. This stage ensures the extraction of maximum power produced by the solar PV array by using an algorithm called maximum power point tracking (MPPT) controller [6] and also step-up the PV voltage produced by PV system to a voltage level required for the VSI. The second power processing unit can be achieved with the help of VSI. This dc-ac converter not only converts dc voltage into the ac voltage but also used for regulating ac power which is injected into the utility grid. This converter with its controller ensures the unity power factor operation with the grid voltages~[7]. The output of VSI is synchronized with the utility grid through the phase lock loop (PLL). A commonly used d-q PLL is used in this work for synchronization purposes. The selection of the proper current control schemes is most important for the overall performance of the grid-connected PV system. The grid current which is injected into the grid could be regulated through the voltage source inverter and maintain a constant dc voltage across the input of the VSI. The VSI also performs the regulation of both real and reactive power which is injected into the utility grid. Numerous current management methods have implemented for the grid-tied voltage source inverter along with the third-order low-pass *LCL* filter. The current control schemes are classified in two ways such as single-loop and dual-loop feedback current management schemes. The effectiveness of the above mentioned current control schemes can be evaluated on the different operating conditions. Many single-loop and multi-loop current control schemes are reported since last few years. However, the previous literature has not more informatics concerning power quality issues and stability problems of the overall system. In renewable energy bases DG system, various current control schemes were mentioned such as hysteresis band , repetitive current controller , predictive current controller and multi-loop current controller [8], [9], [10], and [11]. However, multi-loop control techniques have been gaining popularity due to its simple realization.

Revised Manuscript Received on December 30, 2019.
* Correspondence Author
**Pradeep Kumar Sahu*,** SOEE, KIIT, Deemed to be University, BBSR, India. Email:pksahu.3020@gmail.com
**Satyaranjan Jena,** SOEE, KIIT, Deemed to be University,BBSR, India. Email:srj.kiit@gmail.com
**Gitanjali Dei,** SOEE, KIIT, Deemed to be University,BBSR, India. Email: geetanjaalidei@gmail.com

The mathematical modeling and design of these control schemes for the grid-tied PV plant along-with the third-order filter *LCL* filter are stated in [5].

The parameters of each loops have been estimated in the literature [8]. The single loop current control scheme that is used for regulating the current injected into the utility grid along with the damping register is targeted in [10],~[11]. The performance of numerous control loops which is incorporated with *P*, *PI* and *PID* controllers are demonstrated. By taking the grid current as the feedback in a single-loop control technique, the stability of the overall system has been evaluated in [11]. The internal parameters of the third-order *LCL* filter will be a retardant for the system's operation. Hence, a dual-loop current controller can be employed for regulating grid-current with the existence of filter internal parameter uncertainty [10]. The dual-loop controller for the grid-tied PV plants in the presence of a third-order low-pass filter is given in [2]. The dual power processing steps grid-tied PV plant is reported in the literature [3]. A maximum power point technique based on sliding mode control [6] can be incorporated with the step-up dc to dc converter is employed here to extract maximum available power from the PV panel.

This paper opinions all properties of a voltage source inverter that's integrated with the utility grid. The voltage generated by the PV solar plant is dc type. The dc voltage produced by the PV panel is interfaced with the power conditioning units like dc to dc converter or VSI. The proper controller should be incorporated with the voltage source inverter in the sort of manner that both grid and the VSI output have same voltage magnitude as well as frequency. The various current controllers are discussed in this work to regulate the current which is injected into the grid. A briefly comparison will be made on the basis of its steady-state response, transient response and its overall stability issues.

The remainder of this paper is framed as follows. Section II offers the mathematical modeling of *LCL* filter with the PV plant is given in Section III whereas section III focused on the detailed procedures for designing dual-loop current control techniques. Section IV presents the simulation results to evaluate the performance of the two dual-loop controller. Conclusion of this work is given in Section V.

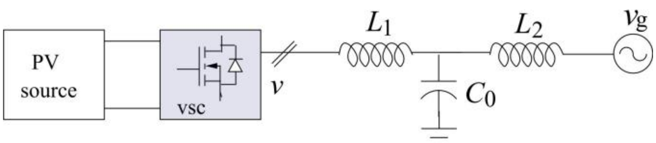


**Fig. 1 . Circuit layout of 1-phase VSI with Low pass filter**

## II. MODELING OF THE SYSTEM

A grid-tied PV generator topology is given in Fig. 1. The grid-tied PV system comprises of a PV module, step-up dc to dc converter, a maximum power point tracker, a VSI to convert the dc power produced by PV system to the ac power as required by the connected load, a third-order low-pass *LCL* filter as well as a grid. Hence, a mathematical model of the grid-tied PV system with a *LCL* filter is essential for anyone for designing a proper controller.

### A. Modeling of PV Cell

The solar energy can be converted into electrical energy with the help of a solar PV module. The smallest part of the solar PV system is solar cells. So it is important to model a solar cell. The solar intensity and the ambient temperature are taken as the input parameter whereas output PV voltage, PV current, and power produced by the solar PV system are taken as the output parameters. There is a single point in the V-I curve where maximum power is available. This point is called maximum power point. The maximum power from the PV cell can be exacted with the help of MPPT algorithm. The dc-dc converter used in the first stage will ensure to extract the maximum available from the PV cell. The current and voltage ripple should be small to operate at the MPP.
The equation of a PV cell is presented by a simple p-n junction diode;

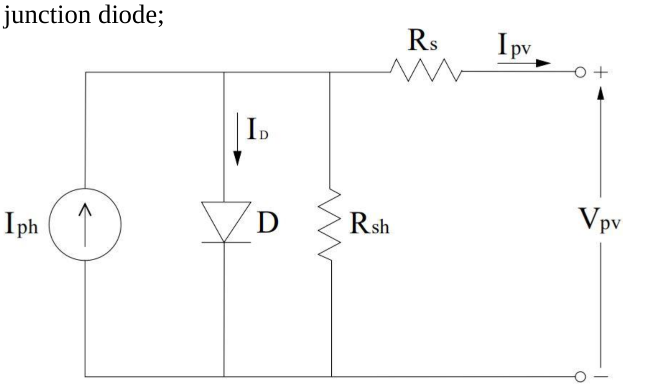


**Fig. 2. Mathematical model of a solar PV cell**

$$I_{PV} = \left( I_{ph} - I_s \left[ \exp^{\frac{q(V+IR_s)}{nkT}} - 1 \right] \right) - \frac{V + IR_s}{R_{sh}} \qquad (1)$$

The PV cell can be developed by considering the (1) which is shown in Fig. 2. The PV cell model consists of a current source shunted with a p-n semiconductor diode. It also has two resistances; one is series resistance and the other one is a shunt resistance. The value of series and shunt resistance is taken as 0.4 ohm and 373 ohm respectively. The maximum safe PV output voltage can be found from open circuit condition and maximum safe PV current can be found from the short circuit condition. The short circuit PV current is $I_{sc}=i_{pv}$ which can be calculated by putting the output voltage zero. Similarly, maximum safe PV voltage known as open- circuit voltage can be calculated by putting current the current zero in (2).

$$V_{OC} = \frac{kT}{q} \ln \frac{I_g + I_{sat}}{I_{sat}} \qquad (2)$$

By taking the series and parallel combination of the PV cell, a PV module can be formed. Let M is the series connection and N is the parallel connection. Therefore, the overall equation of the PV module is represented by

$$I_{PV} = N_p \left( I_{ph} - I_s \left[ \exp^{\frac{q(\frac{V}{N_S})+IR_s}{kT}} - 1 \right] \right) - \frac{\left(\frac{V}{N_S}\right) + \left(\frac{I}{N_P}\right) R_S}{R_{sh}} \qquad (3)$$

In this work, the rating of the PV module is selected as $V_{oc}$ of 86 V and $I_{sc}$ = 24 A.

International Journal of Engineering and Advanced Technology (IJEAT)
ISSN: 2249-8958 (Online), Volume-9 Issue-2, December, 2019

### B. Design of Low Pass Filter.

In the grid-connected PV system, a third-order *LCL* filter is incorporated with the output side of voltage source inverter.

This filter is required for eliminating the high order harmonics which is produced during the switching operation of the inverter. The decoupling features is also contributed by this filter. This low-pass filter topology is given in Fig. 3. Here, $L_1$ is connected with the output side of the VSI and $L_2$ is called the coupling inductor, which is connected with the grid. The capacitance of this low pass filter is denoted as *C*o. In this work, the internal resistance of the low-pass filter can be neglected to avoid complexity. The design of the filter can be done by selecting the exact cut-off frequency. The detailed procedures for modeling the *LCL* low-pass filter are given below.

1. The capacitor of the low-pass filter can be selected by its reactive power. As per the *IEEE* standard, the reactive power level should be less than five percent of the total system power. The large capacitor attenuates more voltage, as a result, there is a decrease in system output voltage.

$$Q \le \frac{0.05P}{3\omega V_m^2} \tag{4}$$

2. The design of $L_1$ can be done by selecting the allowable ripple current of the inverter output current $i_1$. The use of large inductor makes the system bulky and costly. The VSI output inductance can be selected by using the following empirical formula.

$$\Delta I_L = \frac{2V_{dc}}{3L_i f_s} m(m-1) \tag{5}$$

Here *m* is the M.I of the VSI and *fs* is the switching frequency of the VSI. Form the above equation, it can be seen that the maximum ripple current produces for the value of *m*=0.5. By putting this value, the inverter-side inductance can be found as

$$I_1 = \frac{V_{dc}}{6\Delta L_L f_s} \tag{6}$$

3. The design of $L_2$ of *LCL* filter is estimated by taking account of cut-off frequency. of the . The selection of $L_2$ is based on the allowable ripple grid current. However, the $L_2$ can also be estimated by taking r. Here, r is the facor called inverter to grid inductance factor. On applying this method, the value of $L_2$ is given by

$$L_2 = rL_1 \tag{7}$$

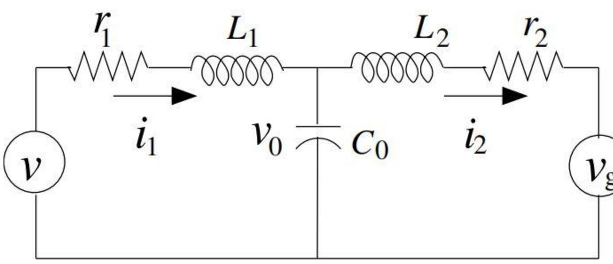


**Fig. 3. Schematic diagram of low-pass filter**

### III. DESIGN OF MULTI-LOOP CURRENT CONTROL SCHEMES

As compared to the single-loop current controller, the dual-loop current controller has better steady-state and the transient response. In this paper, 2 types of two-loop current control schemes are designed and later, their performance will be reduced for the grid-tied VSI. Here, the controller used for this system is to maintain a constant dc voltage across the input side of VSI. It also controls the current to introduce into the grid. Two-types+ of dual-loop current control schemes are briefly discussed here.

### A. Design of Dual-loop Control Scheme with $i_1$ as Inner Loop Feedback Current

This dual-loop current control scheme shown in Fig. 4 consists of two control loops; outer grid current loop and the inner inverter current loop. The function of the outer control loop is to control the grid current and the dynamic performance of the grid-connected PV system is improved by the inner current control loop. The developed and its simplified block diagrams of this controller are shown in Fig. 5 (a) and (b).

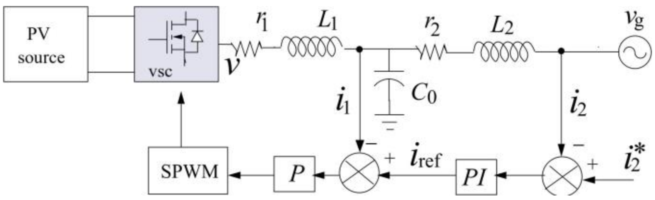


**Fig. 4: Circuit configuration of a grid-connected PV system with $i_1$ as feedback current in inner loop.**

In this dual-control loop, the current error is generated by comparing the injected grid current $i_2$ and the current reference $I^*_2$. A conventional *PI* controller is employed to minimize the grid current error. The reference current for the inner current loop is generated from the outer control loop.

Since the band-width of inner current loop has higher than the outer control loop, a *P*-controller in the inner loop can effectively increase the band-width of this loop. Since both the control loops have different band-width, so these loops are designed separately. The *PI* controller for the outer loop is designed on the basis of cross-over frequency $f_{c1}$ and its resonant frequency $f_r$. The cross-over frequency of the grid-tied PV plant can be chosen as one-fifth of the resonant frequency. From the Bode plot diagram as shown in Fig. 5, at a frequency of 182 Hz, the phase of the open-loop system is equal to -90 degree. The parameters of the *PI* controller are selected in such that a phase margin of 80 degree can be obtained by compensating -10 degree. The detailed procedures for tuning the parameters of PI controller are presented here.

1. The closed loop frequency of the system should be much higher than the cut-off frequency of the *PI* controller.

$$\omega_{cut-off} \ll \omega_{cl} \Rightarrow \frac{K_I}{K_P} \ll \omega_{cl} \tag{8}$$

2 The close loop band-width can be calculated by deriving the transfer function of the closed loop gain at the cross-over frequency.

$$G_{sys(s)s=j\omega_{cl}} = \left(K_p + \frac{K_I}{j\omega_{cl}}\right) G_{i_2}(s)_{s=j\omega_{cl}} \qquad (9)$$

As the value of $K_I/K_p$ is much more than the value of $K_p$ then the term $K_I/j\omega_{cl}$ is negligible in comparison with $K_p$. The above (11) can be rewritten as

$$K_P = \frac{1}{\left|G_{i_2}\right|_{s=j\omega}} \qquad (10)$$

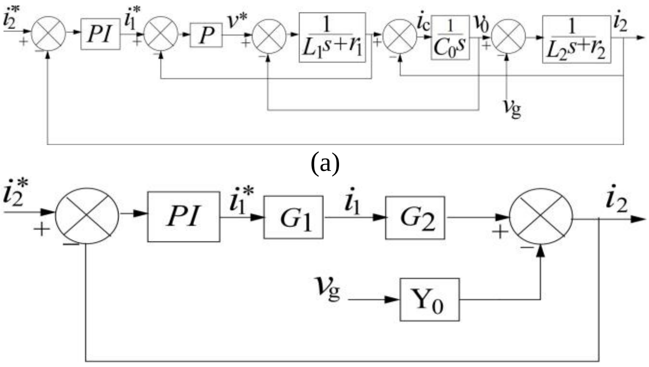


(a)

(b)

**Fig. 5: Dual-loop control diagram with $i_1$ as feedback current in inner loop. (a) control diagram, and (b) simplified diagram.**

2. The phase margin of the system is set as 80 degree, $K_I$ can be calculated as

$$K_I = \frac{K_p\omega_{cl}}{\tan\left(-\pi/18 - \angle G_{I_2}(j\omega_{cl})\right)} \qquad (11)$$

By using the above equations, the $K_p$ and $K_I$ are calculated as 4.086 and 786.05 respectively.

3. The inner P-controller shown in Fig. (5) can be designed on the basis of bandwidth of the inner loop.

$$K_{p(inner)} = \frac{1}{\left|\frac{1}{L_1 s + r_1}\right|_{s=j\omega}} \qquad (12)$$

From the block diagram as shown in Fig. (5), by setting $i_1$=0, the open loop transfer function $Y_0$ is given by

$$Y_0 = \frac{i_2}{v_g} = \frac{1}{L_2 s + r_2 + 1/C_0 s + r_d} \qquad (13)$$

From Fig. 5 (b), the transfer function of $G_1$ and $G_2$ are derived as

$$G_1 = \frac{K_P}{L_1 s + r_1 + K_P} \qquad (14)$$

And

$$G_2 = \frac{i_1}{i_2} = \frac{r_d C_0 s + 1}{L_2 s + (r_d + r_1)C_o s + 1} \qquad (15)$$

### B. Design of Dual-loop Control Scheme with $i_2$ as Inner Loop Feedback Current

Dual-loop current control scheme consists of two loops; the outer loop is the grid-current loop which is required to control $i_2$ and the inner loop is the capacitor current loop which is used for improving the dynamic performance of the system as given in Fig. 6. The developed block diagram of this dual-loop current control scheme is presented in Fig. 7. The current $i_2$ and $i_c$ are sensed from the grid side inductor $L_2$ and the filter capacitor $C_o$. It is noted that the feed-forward control will be included for designing the outer current control loop. The same procedures can be followed for designing both the control loops as highlighted in the previous dual-loop control scheme.

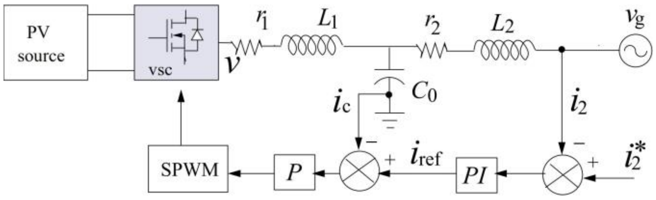


**Fig. 6: Circuit configuration of a grid-connected PV system with capacitor current as feedback current in inner loop.**

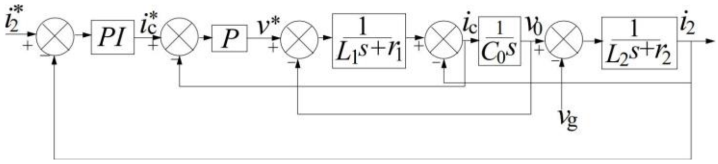


**Fig. 7: Dual-loop control diagram with $i_c$ as feedback current in inner loop.**

**Table-I : Companion of both dual-loop control schemes under Ideal condition**

| Dual-loop control schemes | % THD |
|---|---|
| Outer loop as grid current loop and the inner loop by taking $i_1$ as feedback current | 1.78 % |
| Outer loop as grid current loop and the inner loop by taking $ic$ as feedback current | 3.87 % |

**Table-II : Companion of both dual-loop control schemes under polluted grid condition**

| Dual-loop control schemes | % THD |
|---|---|
| Outer loop as grid current loop and the inner loop by taking $i_1$ as feedback current | 2.64 % |
| Outer loop as grid current loop and the inner loop by taking $ic$ as feedback current | 5.45 % |

## IV. SIMULATION RESULTS

The proposed dual-loop current control techniques are simulated by using the sim-power system toolbox in MATLAB/SIMULINK software. The parameters of the low-pass filter are selected based on the resonant frequency. The resonant frequency for this system is taken as 1 kHz. The control parameters used for two dual-loop current controllers and the system parameter of the grid-connected PV system are; grid voltage = 110V, 50Hz, switching frequency of the inverter fs = 10 kHz, $L_1$ =0.45 mH, $C_0$ = 22 μF, $L_2$=1 mH and the local load of R = 20 ohm.

*Retrieval Number: B4236129219/2019©BEIESP*
*DOI: 10.35940/ijeat.B4236.129219*
*Journal Website: www.ijeat.org*



*Published By:*
*Blue Eyes Intelligence Engineering*
*& Sciences Publication*

International Journal of Engineering and Advanced Technology (IJEAT)
ISSN: 2249-8958 (Online), Volume-9 Issue-2, December, 2019

. The steady-state and dynamic performance of the multi-loop control schemes will be evaluated in this section.

### A. Steady State Performance

The steady-state performance under the ideal grid condition can be analyzed by using the obtained test results. The current $i_2$ injected into the grid and the utility grid voltage $v_g$ of both the dual-loop control schemes are shown in Fig. 8 (a) and (b). The steady-state performance of both the control schemes can be estimated based on the total harmonic distortion (THD). The THD of two control schemes is summarized in Table I. The grid current THD with feedback current $i_1$ as the inner loop is 1.78 % whereas the grid current THD with feedback current $i_c$ as the inner loop is 3.87 %. The grid currents meet the IEEE-519 standard for both the controllers. Moreover, the steady state performance of the dual-loop control scheme with $i_1$as feedback current in the inner loop is better than the dual-loop control scheme with $i_c$ current as feedback in the inner loop.

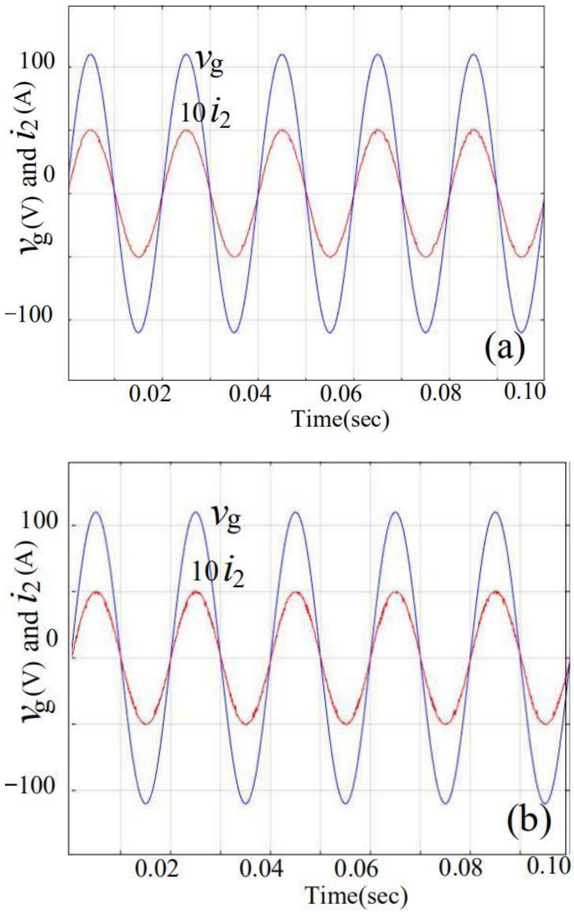


**Fig. 8: Simulated waveforms of $i_2$ and $v_g$ for both the dual-loop control schemes. (a) $i_1$ as feedback current in inner loop, and (b) with capacitor current as feedback current in inner loop.**

### B. Dynamic Performance

First, the performance of both dual-loop control schemes is evaluated under polluted grid condition. Under this condition, the grid has a fundamental component of voltage and low order harmonics components like fifth, seventh and eleventh harmonics. The polluted grid voltage and the grid current for the above two controller are shown in Fig. 9 (a) and (b). The corresponding THD level of both the controller are given in Table II. It is revealed from the figures that the control scheme with inductor current as feedback current in the inner loop gives better results than the dual-loop control scheme with capacitor current feedback as the inner loop. So it conforms the better performance under polluted grid condition.

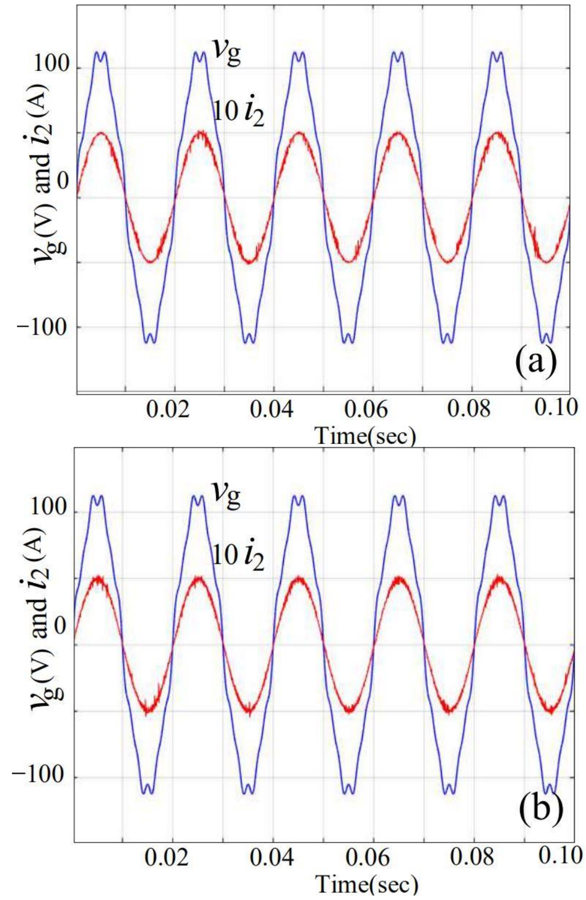


**Fig. 9: Simulated waveforms of $i_2$ and $v_g$ for both the dual-loop control schemes under polluted grid condition. (a) i1 as feedback current in inner loop, and (b) with capacitor current as feedback current in inner loop.**

The dynamic performance of both current controller of the grid-connected PV system under step change in solar insolation level is examined here. The power generated by the PV modules rely on the solar insolation. The test results shown in Fig. 10 (a) and (b) gives the dynamic performance of both the controller under step fluctuation of solar insolation level from 1000 W/m$^2$ to 850 W/m$^2$. From the above results, it is noted that both controllers have tremendous dynamic performance.

## V. CONCLUSION

The PV system can be integrated with the grid with the help of a VSI and *LCL* low-pass filter. The overall performance of the system can be improved significantly by selecting proper parameters of the low-pass filter and choosing the appropriate control scheme. The designing procedures of the low-pass *LCL* filter was presented in this work. Then two types of dual-loop current controllers were designed. The steady state performance of both the dual-loop control techniques were evaluated on the basis of THD.

The dynamic performance of the both the controllers was examined by fluctuating the solar intensity of the PV system. A brief comparison among these controllers was made in this paper. The stability of both the controllers were evaluated. All the test results revealed that the dual-loop control scheme with inductor current feedback as the inner loop has better performance than the dual-loop control scheme with capacitor current feedback as the inner loop.

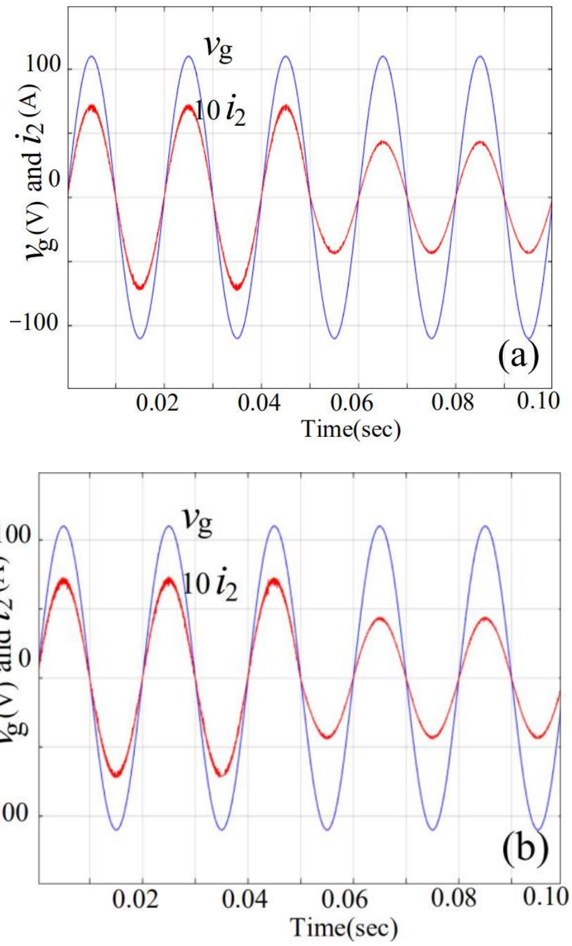


**Fig. 10: Dynamic response of both the controller under sudden fluctuation of solar irradiance.**

## REFERENCES

1. B. K. Bose, "Global Warming: Energy, Environmental Pollution, and the Impact of Power Electronics," in IEEE Industrial Electronics Magazine, vol. 4, no. 1, pp. 6-17, March 2010.
2. Y. Wu, J. Lin and H. Lin, "Standards and Guidelines for Grid-Connected Photovoltaic Generation Systems: A Review and Comparison," in IEEE Transactions on Industry Applications, vol. 53, no. 4, pp. 3205-3216, July-Aug. 2017.
3. Mohan, Ned, T. M. Undeland, and W. P. Robbins. Power electronics: converters, applications, and design. John wiley & sons, 2003.
4. N. Tripathi, A. Singh and T. Hanamoto, "Design and control of LCL filter interfaced grid connected solar photovoltaic (SPV) system using power balance theory", International Journal of Electrical Power & Energy Systems, Volume 69, 2015, Pages 264-272.
5. H. Cha and T. Vu, "Comparative analysis of low-pass output filter for single-phase grid-connected Photovoltaic inverter," 2010 Twenty-Fifth Annual IEEE Applied Power Electronics Conference and Exposition (APEC), Palm Springs, CA, 2010, pp. 1659-1665.
6. Maity and P. K. Sahu, "Modeling and Analysis of a Fast and Robust Module-Integrated Analog Photovoltaic MPP Tracker," in IEEE Transactions on Power Electronics, vol. 31, no. 1, pp. 280-291, Jan. 2016.
7. M. Calais, J. Myrzik, T. Spooner and V. G. Agelidis, "Inverters for single-phase grid connected photovoltaic systems-an overview," 2002 IEEE 33rd Annual IEEE Power Electronics Specialists Conference. Proceedings (Cat. No.02CH37289), Cairns, Qld., Australia, 2002, pp. 1995-2000 vol.4.
8. K, Palanisamy K, Vijayakumar D. "Recent advances and control techniques in grid connected PV system–A review". International Journal of Renewable Energy Research. 2016 Sep 6;6(3):1031-49.
9. M. Golestan "Control strategies for single-phase grid integration of small-scale renewable energy sources: A review". Renewable and Sustainable energy reviews. 2012 Sep 1;16(7):4982-93.
10. Teodorescu R, Blaabjerg F, Liserre M, Loh PC. Proportional-resonant controllers and filters for grid-connected voltage-source converters. IEE Proceedings-Electric Power Applications. 2006 Sep 1;153(5):750-62.
11. Athari, M. Niroomand, M. Ataei "Review and classification of control systems in grid-tied inverters". Renewable and Sustainable Energy Reviews. 2017 May 1;72:1167-76.

## AUTHORS PROFILE

**Dr. Pradeep Kumar Sahu**, received his Ph.D. degree form NIT, Rourkela in 2016. He is currently working as Associate professor in School of Electrical Engineering,KIIT Deemed to be University Bhubaneswar, Odisha. His current research interests include modeling and control of power electronic converters, nonlinear control and power quality improvement in Distribution Generation systems.

**Dr. Satyaranjan Jena,** received his Ph.D. degree form KIIT,demmed to be University in 2016. He is currently working as an assistant professor in School of Electrical Engineering,KIIT Deemed to be University Bhubaneswar,Odisha. He has teaching experience of 15 years and research experience of 7 years. His current research interests includes grid Integartion of renewables, Softcomputindg and Power Electronics.

**Geetanjali Dei,** received her B.E. Degree from Department of Electrical Engineering; University College of Engineering, Burla, Orissa in 2001.She obtained her M.Tech. degree in power system engineering from V.S.S.U.T, Burla in 2010. She is working as assistant professor in Kalinga institute of industrial Technology, Deemed to be university Orissa. She has been teaching for the last 15 years. Her research areas of interest are soft computing, power system operation and control and automatic generation control.